ANALYTICAL AND COMPUTATIONAL STUDIES ON THE INTERACTION OF A SUM AND A DIFFERENCE RESONANCE

H. Meier (*) **and K. R. Symon** (**)

Midwestern Universities Research Association, Madison, Wis. (***)

(presented by K. R. Symon)

I. INTRODUCTION

Analytical theories of the behavior of non-linear motion in two degrees of freedom near a coupling resonance lead to the conclusion [1], that near a sum resonance, there are limiting amplitudes, depending on the distance from the resonance and vanishing at the resonance, above which the coupled motion is unstable. In contrast, near a difference resonance, there are corresponding amplitudes above which the two degrees of freedom become strongly coupled and exchange " energy ", but the analytic theory predicts that the motion is stable. However, computed orbits in accelerators near difference resonances, and particularly near the " Walkinshaw resonance " $\nu_x - 2\nu_y = 0$, have often shown [3] actual instabilities in addition to the expected strong coupling. Hagedorn [2] has offered a possible explanation of these effects as due to the presence of a pass through the potential energy hills surrounding the equilibrium point, which is not accessible to a particle moving along the x-axis or y-axis alone, even though the energy is high enough, but becomes accessible when the x and y motions are strongly coupled. We have considered the more general possibility that the paradoxical instabilities may be due to the presence of another nearby resonance in addition to the difference resonance which produces the coupling. To this end, we have chosen to consider motions for which the working point ν_x, ν_y lies near the sum resonance $\nu_x+2\nu_y = N$ as well as the difference resonance $\nu_x-2\nu_y = 0$. (N = number of sectors around the accelerator.) We will develop below an analytical theory of the motion, and present in addition results of fairly extensive digital computations of orbits. In order to make rapid calculations through many sectors, as well as to simplify the analytic theory, we have chosen a Hamiltonian of the simplest form which exhibits the resonance in question and which at the same time lends itself to rapid digital computation. We are able to give a partial though not a complete analytic solution to the problem. The analytic results are confirmed and extended by the results of digital computation, so that we now believe we have a fairly complete understanding of the phenomena which occur. Our explanation of the paradoxical results will be related to Hagedorn's. In our terminology, Hagedorn suggests a possible interaction between the integral resonance lines $\nu_x = 0$ and $\nu_y = 0$ and the difference resonance $\nu_x - 2\nu_y = 0$ which they intersect. This can certainly occur, but more generally the interaction may also be with other resonance lines.

The following Hamiltonian will be used for the study of the motion of a particle near the intersection (see Fig. 1) of the $\nu_x-2\nu_y = 0$ and $\nu_x+2\nu_y = N$ resonance lines, $\left(\nu_x = \frac{N}{2}, \quad \nu_y = \frac{N}{4}\right)$:

$$H = \frac{\nu_x}{2}(p_x^2+x^2)+\frac{\nu_y}{2}(p_y^2+y^2)-\frac{\lambda}{2}xy^2\Delta(N\theta). \tag{1}$$

(*) University of Wisconsin, Madison, Wis.

(**) On leave from University of Wisconsin.

(***) Supported by the United States Atomic Energy Commission.

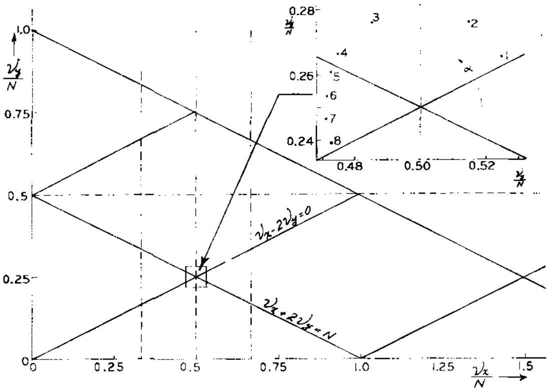

Fig. 1 Resonance diagram showing the resonances $\nu_x - 2\nu_y = 0$, $\nu_x + 2\nu_y = N$, and other important resonances influencing the motion. Insert shows working points for which digital computations were made.

$\Delta(N\theta)$ is a periodic Dirac delta function of period $2\pi/N$,

$$\Delta(N\theta) = 0 \text{ for } \theta \neq \frac{2\pi n}{N},$$

and

$$\int_{\frac{2\pi n}{N}-\varepsilon}^{\frac{2\pi n}{N}+\varepsilon} d\theta\, \Delta(N\theta) = 1,$$

where n is an integer. The horizontal and vertical displacements of the particle from the equilibrium orbit are represented by the variables x and y; the conjugate momenta, by p_x and p_y. In general the quadratic terms of an accelerator Hamiltonian will contain coefficients that are periodic in θ; however, a canonical transformation exists [1] which will transform the accelerator Hamiltonian into a form whose quadratic terms are the same as Eq. (1).

The lowest order term in an accelerator Hamiltonian which produces resonances in the neighborhood of $\nu_x = N/2$, $\nu_y = N/4$ is $f(N\theta)\, xy^2$, where $f(N\theta)$ is periodic in θ with period $2\pi/N$. In Eq. (1), $f(N\theta)$ has been chosen as $-\lambda\Delta(N\theta)/2$. This makes it possible to express the solution of the equations of motion in the form of an algebraic transformation which will carry the particle from

$$\theta = \frac{2\pi n}{N} \text{ to } \theta = \frac{2\pi(n+1)}{N},$$

i.e., through one sector. The function $\Delta(N\theta)$ probably excites higher order resonances more than a more realistic $f(N\theta)$ for an accelerator, since the higher harmonics of $f(N\theta)$ will go to zero while the higher harmonics of $\Delta(N\theta)$ do not. However, the qualitative features of the motion should be the same.

It has been customary (although not necessary) in computer studies of coupled motion, to compute orbits which begin with very small initial amplitudes of y-motion, and to investigate the behavior of the solution as a function of initial x-amplitude; (usually $p_x = 0$ also initially). We shall adhere to this procedure in this paper. Under these conditions, it is found both analytically and by computation that near the difference resonance there is a threshold x-amplitude x_t depending on the distance from the resonance and vanishing at the resonance, above which the y and x motions are strongly coupled and the y motion begins to grow exponentially. According to analytical theory, the y motion should reach a maximum amplitude and decline again periodically as the "energy" is exchanged between x and y. In computed orbits, the y motion is sometimes found also to be unstable, either immediately or after a number of oscillations in amplitude. Near a sum resonance, both analysis and computation agree that there is a stability limit x_s above which the motion is unstable. We seek to study and account for these phenomena in this paper.

II. THE ALGEBRAIC TRANSFORMATION

From the Hamiltonian (1)

$$x' = \frac{\partial H}{\partial p_x} = \nu_x p_x,$$

$$p'_x = -\frac{\partial H}{\partial x} = -\nu_x x + \frac{\lambda}{2} y^2 \Delta(N\theta),$$

and

$$y' = \frac{\partial H}{\partial p_y} = \nu_y p_y,$$

$$p'_y = -\frac{\partial H}{\partial y} = -\nu_y y + \lambda x y \Delta(N\theta).$$

Since the delta function occurs at $\theta = 2\pi n/N$ the variables p_x, p_y have discontinuities at these points, while x, y are continuous:

$$x\left(\frac{2\pi n}{N}+\right)=x\left(\frac{2\pi n}{N}-\right),$$

$$p_x\left(\frac{2\pi n}{N}+\right)=p_x\left(\frac{2\pi n}{N}-\right)+\frac{\lambda}{2}y^2\left(\frac{2\pi n}{N}\right),$$

$$y\left(\frac{2\pi n}{N}+\right)=y\left(\frac{2\pi n}{N}-\right),\tag{2}$$

$$p_y\left(\frac{2\pi n}{N}+\right)=p_y\left(\frac{2\pi n}{N}-\right)+\lambda x\left(\frac{2\pi n}{N}\right)y\left(\frac{2\pi n}{N}\right).$$

For

$$\frac{2\pi n}{N}<\theta<\frac{2\pi(n+1)}{N},$$

$$x''=\nu_x p_x'=-\nu_x^2 x,$$

and

$$x\left(\frac{2\pi(n+1)}{N}-\right)=x\left(\frac{2\pi n}{N}+\right)\cos\frac{2\pi\nu_x}{N}+ +p_x\left(\frac{2\pi n}{N}+\right)\sin\frac{2\pi\nu_x}{N},$$

$$p_x\left(\frac{2\pi(n+1)}{N}-\right)=-x\left(\frac{2\pi n}{N}+\right)\sin\frac{2\pi\nu_x}{N}+ +p_x\left(\frac{2\pi n}{N}+\right)\cos\frac{2\pi\nu_x}{N}.$$

Finally, we have the transformation through a sector

from $\theta=\dfrac{2\pi n}{N}-$ to $\dfrac{2\pi(n+1)}{N}-$:

$$x\Big|_{\frac{2\pi(n+1)}{N}-}=\left[x\cos\frac{2\pi\nu_x}{N}+p_x\sin\frac{2\pi\nu_x}{N}+ +\frac{\lambda}{2}y^2\sin\frac{2\pi\nu_x}{N}\right]_{\frac{2\pi n}{N}-},\tag{3a}$$

$$p_x\Big|_{\frac{2\pi(n+1)}{N}-}=\left[-x\sin\frac{2\pi\nu_x}{N}+p_x\cos\frac{2\pi\nu_x}{N}+ +\frac{\lambda}{2}y^2\cos\frac{2\pi\nu_x}{N}\right]_{\frac{2\pi n}{N}-},$$

where all variables are evaluated just before the delta function. In a similar manner

$$y\Big|_{\frac{2\pi(n+1)}{N}-}=\left[y\cos\frac{2\pi\nu_y}{N}+p_y\sin\frac{2\pi\nu_y}{N}+ +\lambda xy\sin\frac{2\pi\nu_y}{N}\right]_{\frac{2\pi n}{N}-},\tag{3b}$$

$$p_y\Big|_{\frac{2\pi(n+1)}{N}-}=\left[-y\sin\frac{2\pi\nu_y}{N}+p_y\cos\frac{2\pi\nu_y}{N}+ +\lambda xy\cos\frac{2\pi\nu_y}{N}\right]_{\frac{2\pi n}{N}-}.$$

With these equations a computer can calculate x, y, p_x, and p_y through a large number of sectors, several thousand times faster than if it had to do the calculation by solving the differential equations of motion numerically. An orbit can be followed through of the order of a million sectors in about an hour with the MURA IBM-704 computer. A number of computer runs have been performed based on Eqs. (3). These results will be presented in Section IV, where they will be compared with the analytic results that will be derived in Section III.

III. ANALYTIC TREATMENT

The analytic treatment of the problem will be based on methods developed by J. Moser [4].

Since

$$\Delta(N\theta)=\frac{N}{2\pi}\sum_{m=-\infty}^{\infty}e^{imN\theta},$$

then

$$H=\frac{\nu_x}{2}(p_x^2+x^2)+\frac{\nu_y}{2}(p_y^2+y^2)-\frac{\lambda N}{4\pi}xy^2\sum_{m=-\infty}^{m=\infty}e^{imN\theta}.\tag{4}$$

Let

$$x=\rho_{x_0}^{\frac{1}{2}}\cos\gamma_{x_0},\quad p_x=\rho_{x_0}^{\frac{1}{2}}\sin\gamma_{x_0},$$
$$y=\rho_{y_0}^{\frac{1}{2}}\cos\gamma_{y_0},\quad p_y=\rho_{y_0}^{\frac{1}{2}}\sin\gamma_{y_0}.\tag{5}$$

The variables $\rho_{x_0}^{\frac{1}{2}}$, γ_{x_0} are polar co-ordinates in the x, p_x-phase plane, and likewise the y-variables. But also ρ_{x_0}, γ_{x_0}, ρ_{y_0}, γ_{y_0} are canonical variables with momenta ρ_{x_0}, ρ_{y_0}. The Hamiltonian is $K_0=-2H$:

$$K_0 = -\nu_x\rho_{x_o} - \nu_y\rho_{y_o} + \frac{\lambda N}{2\pi}\rho_{x_o}^{\frac{1}{2}}\rho_{y_o}\cos\gamma_{x_o}\cos^2\gamma_{y_o}\sum_{m=-\infty}^{m=\infty} e^{imN\theta},$$

or

$$K_0 = -\nu_x\rho_{x_o} - \nu_y\rho_{y_o} + \frac{\lambda N}{8\pi}\rho_{x_o}^{\frac{1}{2}}\rho_{y_o}\sum_{m=-\infty}^{\infty}\left[2\cos(\gamma_{x_o}+mN\theta)+\right.$$

$$\left.+\cos(\gamma_{x_o}+2\gamma_{y_o}+mN\theta)+\cos(\gamma_{x_o}-2\gamma_{y_o}+mN\theta)\right]. \tag{6}$$

We now make a transformation $\rho_{x_o}, \gamma_{x_o}, \rho_{y_o}, \gamma_{y_o} \to \rho_x, \gamma_x, \rho_y, \gamma_y$ be means of the generating function

$$S = \gamma_{x_o}\rho_x + \gamma_{y_o}\rho_y - \frac{\lambda N}{8\pi}\rho_x^{\frac{1}{2}}\rho_y\left[\sum_{\substack{m=-\infty \\ m\neq 1}}^{\infty}\frac{\sin(\gamma_{x_o}+2\gamma_{y_o}+mN\theta)}{(mN-\nu_x-2\nu_y)}+\right. \tag{7}$$

$$\left.+\sum_{\substack{m=-\infty \\ m\neq 0}}^{\infty}\frac{\sin(\gamma_{x_o}-2\gamma_{y_o}+mN\theta)}{(mN-\nu_x+2\nu_y)}+\sum_{m=-\infty}^{\infty}2\frac{\sin(\gamma_{x_o}+mN\theta)}{(mN-\nu_x)}\right],$$

to obtain the new Hamiltonian

$$K = -\nu_x\rho_x - \nu_y\rho_y + \frac{\lambda N}{8\pi}\rho_x^{\frac{1}{2}}\rho_y[\cos(\gamma_x+2\gamma_y+N\theta)+\cos(\gamma_x-2\gamma_y)]+\ldots, \tag{8}$$

where the dots contains terms of higher order than $\rho_x^{\frac{1}{2}}\,\rho_y$. The coefficients of these terms are small if (ν_x, ν_y) is closer to $(N/2, N/4)$ than to any other intersection of resonance lines excited by $-\lambda xy^2\Delta\,(N\theta)/2$. Fig. 1 shows the lines excited by this term, (solid lines), as well as other nearby resonances which are important in accelerators and may be excited by terms of other forms which we have not included. Some of these resonances are driven by higher order terms represented by the dots in Eq. (8).

A typical term, for example, appearing in K which might be important near the point $\nu_x = N/2$, $\nu_y = N/4$ is approximately

$$-\frac{\lambda^2}{768}\left[\frac{\varepsilon_-(1-0.342\varepsilon_-^2)}{(1-\varepsilon_-^2)}+\frac{\varepsilon_+(1-0.342\varepsilon_+^2)}{(1-\varepsilon_+^2)}\right]\rho_y^2\cos(4\gamma_y+N\theta),$$

where

$$\varepsilon_+ = \nu_x + 2\nu_y - N,$$

$$\varepsilon_- = \nu_x - 2\nu_y$$

measure the distance of the working point ν_x, ν_y from the sum and the difference resonance. Note that since $\varepsilon_+ = \varepsilon_- = 0$ for $\nu_x = N/2$, $\nu_y = N/4$, the term vanishes at this point. This term would tend to drive the resonance $\nu_y = N/4$, which passes through $\nu_x = N/2$, $\nu_y = N/4$.

It will be assumed that ρ_x and ρ_y are small enough, and the operating point is close enough to $\nu_x = N/2$, $\nu_y = N/4$ so that all terms in K of order ρ^2 and higher can be neglected, and K will be set equal to

$$K = -\nu_x\rho_x - \nu_y\rho_y + \frac{\lambda N}{8\pi}\rho_x^{\frac{1}{2}}\rho_y[\cos(\gamma_x+2\gamma_y+N\theta)+\cos(\gamma_x-2\gamma_y)]. \tag{9}$$

Note that we can obtain Eq. (9) immediately simply by neglecting all non-linear terms in Eq. (6) except those which excite the two resonances of interest. This is equivalent to identifying ρ_{x_o}, γ_{x_o}, ρ_{y_o}, γ_{y_o} with ρ_x, γ_x, ρ_y, γ_y, that is, neglecting the higher order terms in the transformation given by Eq. (7). A second canonical transformation $\rho_x, \gamma_x, \rho_y, \gamma_y \to \underline{\rho_x}, \underline{\gamma_x}, \underline{\rho_y}, \underline{\gamma_y}$ will now be performed using the generating function

$$F = \underline{\rho_x}\left(\gamma_x + \frac{N}{2}\theta\right) + \underline{\rho_y}\left(\gamma_y + \frac{N}{4}\theta\right). \tag{10}$$

This is a rotation in the x-phase plane at a rate 'ν_x' $= N/2$ and in the y-phase plane at 'ν_y' $= -N/4$:

$$\underline{\rho_x} = \rho_x, \underline{\gamma_x} = \gamma_x + \frac{N}{2}\theta,$$

$$\underline{\rho_y} = \rho_y, \underline{\gamma_y} = \gamma_y + \frac{N}{4}\theta,$$

and leads to a Hamiltonian independent of θ:

$$\underline{K} = -\left(\nu_x - \frac{N}{2}\right)\underline{\rho_x} - \left(\nu_y - \frac{N}{4}\right)\underline{\rho_y} + \frac{\lambda N}{8\pi}\underline{\rho_x}^{\frac{1}{2}}\underline{\rho_y}[\cos(\underline{\gamma_x}+2\underline{\gamma_y})+\cos(\underline{\gamma_x}-2\underline{\gamma_y})]. \tag{11}$$

Using the generating functions (7) and (10) along with Equation (5) it is found that x and p_x have the forms, at $\theta = 8\pi\eta/N$,

$$x = \underline{\rho_x}^{\frac{1}{2}}\cos\underline{\gamma_x} + \underline{\rho_y}f(\underline{\gamma_x}, \underline{\gamma_y}) + \ldots,$$

$$p_x = \underline{\rho_x}^{\frac{1}{2}}\sin\underline{\gamma_x} + \underline{\rho_y}g(\underline{\gamma_x}, \underline{\gamma_y}) + \ldots,$$

where the dots represent terms of higher order in ρ_x and ρ_y.

The initial conditions that are of interest in this paper have $\rho_y \ll \rho_x$, and the only final conditions of interest are whether ρ_x and ρ_y grow and remain finite or not. Consequently the initial x and p_x can be taken correct to order ρ_x as

$$x = \underline{\rho}_x^{\frac{1}{2}} \cos \underline{\gamma}_x$$

$$p_x = \underline{\rho}_x^{\frac{1}{2}} \sin \underline{\gamma}_x \,. \tag{12}$$

It is not necessary to know y and p_y in terms of $\underline{\rho}_x$, $\underline{\rho}_y$, $\underline{\gamma}_x$, and $\underline{\gamma}_y$. The only information needed is that if $\underline{\rho}_y$ is very small then y and p_y are very small, and conversely. However, to order $\rho_x^{\frac{1}{2}}$, $\rho_y^{\frac{1}{2}}$, we may identify $\underline{\rho}_x$, $\underline{\gamma}_x$, $\underline{\rho}_y$, $\underline{\gamma}_y$ with ρ_{x_o}, γ_{x_o}, ρ_{y_o}, γ_{y_o} in Eqs. (5) at $\theta = 8\pi n/N$.

Since $\underline{K}$ does not contain θ explicitly, it is a constant of the motion. $\underline{K}$ can also be written in the form

$$\underline{K} = -\varepsilon_x\underline{\rho}_x - \varepsilon_y\underline{\rho}_y + \frac{\lambda N}{4\pi}\underline{\rho}_x^{\frac{1}{2}}\underline{\rho}_y \cos \underline{\gamma}_x \cos 2\underline{\gamma}_y \,, \tag{13a}$$

where

$$\varepsilon_x = \nu_x - \frac{N}{2}\,, \quad \varepsilon_y = \nu_y - \frac{N}{4}\,.$$

It is convenient to reintroduce rectangular co-ordinates in the rotating x- and y-phase planes:

$$X = \underline{\rho}_x^{\frac{1}{2}} \cos \underline{\gamma}_x\,, \quad Y = \underline{\rho}_y^{\frac{1}{2}} \cos \underline{\gamma}_y\,,$$

$$P_x = \underline{\rho}_x^{\frac{1}{2}} \sin \underline{\gamma}_x\,, \quad P_y = \underline{\rho}_y^{\frac{1}{2}} \sin \underline{\gamma}_y\,.$$

In these rectangular coordinates,

$$-\tfrac{1}{2}\underline{K} = \tfrac{1}{2}\varepsilon_x P_x^2 + \tfrac{1}{2}\left(\varepsilon_y + \frac{\lambda N}{4\pi}X\right)P_y^2 + \tfrac{1}{2}\varepsilon_x X^2 + \tfrac{1}{2}\varepsilon_y Y^2 - \frac{\lambda N}{8\pi} X Y^2. \tag{13b}$$

Let us first take ε_x, ε_y in the first quadrant (both positive, see insert Fig. 1). Eq. (13b) can be regarded as a Hamiltonian in which the first two terms represent a positive definite kinetic energy $\left(\text{if } X > -\dfrac{4\pi\varepsilon_y}{\lambda N}\right)$, and the last three, a potential energy $V(X, Y)$. The potential $V(X, Y)$ contains a valley from which the particle may exit through either of two passes whose saddle points lie at

$$X_l = \frac{4\pi}{\lambda N}\varepsilon_y\,, \quad Y_l = \pm\frac{4\pi}{\lambda N}(2\varepsilon_x\varepsilon_y)^{\frac{1}{2}},$$

and the minimum energy for crossing either pass is

$$-\tfrac{1}{2}K_l = \tfrac{1}{2}\varepsilon_x\varepsilon_y{}^2\left(\frac{4\pi}{\lambda N}\right)^2.$$

For negligible initial y-amplitude, and $p_x = 0$ initially, the limiting x-amplitude for which the energy is sufficient to cross the pass is

$$|x_l| = X_l = \frac{4\pi}{\lambda N}\left(\nu_y - \frac{N}{4}\right). \tag{14}$$

Note that at this amplitude, the "mass" of the y-motion can become zero and at greater energies the particle can escape through the point $-X_l$, $Y = 0$ by acquiring a negative y-mass, as well as through the passes at X_l, $\pm Y_l$.

Our analysis does not indicate under what conditions the particle will escape if initially $|x| > X_l$, but only that if $|x| < X_l$ it surely cannot escape (to the extent that the Hamiltonian (13) is a valid approximation). We shall have more to say later as to when it actually does escape. In view of the asymptotically convergent character of the Moser-Birkhoff solution by successive transformations, we may expect that our statements based on the Hamiltonian (13) are valid for very long times for small enough amplitudes. Since we find a structure of the dynamical motions with a scale proportional to the distances from the resonances, by going near enough the fixed point, we may expect to find this structure reproduced as accurately as we wish.

If we now consider the second quadrant ($\varepsilon_x < 0$, $\varepsilon_x > 0$) we readily observe that our Hamiltonian (13b) is indefinite even near the origin, and we can find curves of constant $K = 0$ connecting the origin with infinity. We can therefore say nothing about the stability in this case, except that it is "energetically" possible with the Hamiltonian (13b) for the particle to escape with any initial amplitude.

We will prove later a theorem of corresponding motions, one corollary of which is that motions in the third and fourth quadrants are identical with those for corresponding working points in the first and second quadrants.

We can give a complete solution for the motion if we treat the effect of a single resonance separately. Let us take the difference resonance, $\nu_x - 2\nu_y = 0$. We could transform away the term in the Hamiltonian (11) which drives the sum resonance, or, more easily, simply neglect it, which is equivalent to equating the new and old variables in the transformation:

$$\underline{K} = -\left(\nu_x-\frac{N}{2}\right)\underline{\rho}_x-\left(\nu_y-\frac{N}{2}\right)\underline{\rho}_y+\frac{\lambda N}{8\pi}\underline{\rho}_x^{\frac{1}{2}}\underline{\rho}_y\cos(\underline{\gamma}_x-2\underline{\gamma}_y). \tag{15}$$

Now the generating function

$$S = \rho_1(\underline{\gamma}_x-2\underline{\gamma}_y)+\rho_2\underline{\gamma}_y$$

leads to the transformation

$$\underline{\rho}_x = \frac{\partial S}{\partial \underline{\gamma}_x} = \rho_1, \quad \underline{\rho}_y = \rho_2-2\rho_1,$$

$$\gamma_1 = \underline{\gamma}_x-2\underline{\gamma}_y, \qquad \gamma_2 = \underline{\gamma}_y,$$

$$K_1 = -(\nu_x-2\nu_y)\rho_1-\left(\nu_y-\frac{N}{4}\right)\rho_2+ \\ +\frac{\lambda N}{8\pi}\rho_1^{\frac{1}{2}}(\rho_2-2\rho_1)\cos\gamma_1. \tag{16}$$

Since γ_2 is ignorable,

$$\frac{d\rho_2}{d\theta} = -\frac{\partial K_1}{\partial \gamma_2} = 0,$$

ρ_2 is a constant, and terms containing ρ_2 only can be absorbed in K_1, since K_1 is also a constant of the motion. K_1 can be written

$$K_1 = -\varepsilon_-\rho_1+\frac{\lambda N}{8\pi}\rho_1^{\frac{1}{2}}(\rho_2-2\rho_1)\cos\gamma_1, \tag{17}$$

where ε_- measures the distance from the resonance, as defined previously. We finally transform back to rectangular variables

$$X = \rho_1^{\frac{1}{2}}\cos\gamma_1,$$
$$P_x = \rho_1^{\frac{1}{2}}\sin\gamma_1, \tag{18}$$

and

$$H_1 = -\tfrac{1}{2}K_1 = \tfrac{1}{2}\varepsilon_-(X^2+P_x^2)-\frac{\lambda N}{16\pi}X(\rho_2-2X^2-2P_x^2). \tag{19}$$

We plot in Fig. 2, curves of constant K, in the ρ_1, γ_1-plane. From Equation (16) it can be seen that the physically allowed phase points lie within the circle

$$\rho_1 \leq \tfrac{1}{2}\rho_2. \tag{20}$$

We distinguish two cases.

Case (a) $\qquad \rho_2 < \dfrac{32\pi^2}{\lambda^2N^2}\varepsilon_-^2$

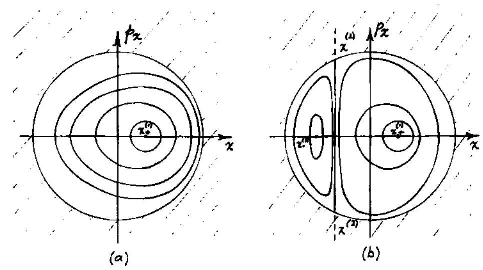

Fig. 2 Phase plots for the Walkinshaw difference resonance $\nu_x-2\nu_y = 0$. Shaded region is excluded as non-physical. (a) Below threshold. (b) Above threshold.

The phase plot appears as in Fig. 2a, where

$$X_+^{(1)} = \frac{-\varepsilon_-+\left[\varepsilon_-^2+\dfrac{3\lambda^2N^2}{32\pi^2}\right]^{\frac{1}{2}}}{3\lambda N/4\pi} \tag{21}$$

Case (b) $\qquad \rho_2 > \dfrac{32\pi^2}{\lambda^2N^2}\varepsilon_-^2.$

In this case four fixed points are present and the phase plot appears as in Fig. 2 b.

The fixed points are given by

$$X_\pm^{(1)} = \frac{-\varepsilon_-\pm\left[\varepsilon_-^2+\dfrac{3\lambda^2N^2}{32\pi^2}\right]^{\frac{1}{2}}}{3\lambda N/4\pi} \tag{22}$$

$$P_x^{(1)} = 0 \tag{23}$$

$$X^{(2)} = -\frac{4\pi\varepsilon_-}{\lambda N} \tag{24}$$

$$P_{x\pm}^{(2)} = \pm\left[\tfrac{1}{2}\rho^2-\frac{16\pi^2}{\lambda^2N^2}\varepsilon_-^2\right]^{\frac{1}{2}} \tag{25}$$

From Eq. (16) we see that if we take as initial conditions $\rho_y \ll \rho_x$, the phase point will follow a path which is very close to the circle $\rho_1 = \frac{1}{2}\rho_2$. In diagram 2a the path remains close to the circle and there is no change in the nature of the motion. In diagram 2b there is a sudden change leading to y growth at the fixed points $P_{x\pm}^{(a)}$, $X^{(2)}$. Hence the condition for y growth is that for $\rho_y \ll \rho_x$ initially,

$$\rho_1 \doteq \tfrac{1}{2}\rho_2 > \frac{16\pi^2}{\lambda^2N^2}(\nu_x-2\nu_y)^2,$$

and if ρ_x is initially zero, the threshold for y-growth is

$$x_t = \rho_x^{\frac{1}{2}} = \rho_1^{\frac{1}{2}} = \frac{4\pi}{\lambda N}\left|\nu_x-2\nu_y\right|. \tag{26}$$

This means that if one starts the motion with y and p_y very small, $p_x = 0$, and $|x| < x_t$, then y will remain very small. However, if $|x| > x_t$, then no matter how small y is, so long as it is not zero, it will grow large. Note that the y amplitude does not grow indefinitely but exhibits a periodic oscillation to a finite amplitude which can be calculated :

$$\rho_{y\,\max}^{\frac{1}{2}} = [2(x_0^2 - x_t^2)]^{\frac{1}{2}}, \tag{27}$$

where χ_0 is the initial x-amplitude. This result is confirmed by numerical computations in appropriate cases, as we shall see.

In the case where the sum resonance, $\nu_x + 2\nu_y = N$ acts alone, we can follow a similar procedure and again give a complete description of the motion. The phase plots in appropriate co-ordinates are in fact essentially the outside (cross hatched) regions in Figs. 2. We will limit ourselves to quoting the result for the case of interest, namely, very small initial y-amplitude, and p_x initially zero, for which we find a stability limit

$$x_s = \frac{4\pi}{\lambda N} |\nu_x + 2\nu_y - N| . \tag{28}$$

If initially $|x| < x_s$, the motion is stable, but if $|x| > x_s$, the y-amplitude and likewise the x-amplitude grow without limit.

If the Hamiltonian given by Eq. (10) were exact, a theorem of corresponding motions would hold. Let

$$K = -\alpha\varepsilon_x\rho_x - \alpha\varepsilon_y\rho_y + A\rho_x^{\frac{1}{2}}\rho_y[\cos(\gamma_x + 2\gamma_y) + + \cos(\gamma_x - 2\gamma_y)] . \tag{29}$$

Now let

$$\theta = \alpha^{-1}\underline{\theta}, \quad \rho_x = \alpha^2 \underline{\rho_x}, \quad \gamma_x = \underline{\gamma_x}$$
$$\frac{d}{d\theta} = \alpha \frac{d}{d\underline{\theta}}, \quad \rho_y = \alpha^2 \underline{\rho_y}, \quad \gamma_y = \underline{\gamma_y} . \tag{30}$$

Then it is readily verified by direct calculation that the equations of motion given by the Hamiltonian (29) are equivalent to those which can be derived from the Hamiltonian

$$\underline{K} = -\varepsilon_x\underline{\rho_x} - \varepsilon_y\underline{\rho_y} + A\underline{\rho_x}^{\frac{1}{2}}\underline{\rho_y}[\cos(\underline{\gamma_x} + 2\underline{\gamma_y}) + \cos(\underline{\gamma_x} - 2\underline{\gamma_y})] \tag{31}$$

This means that there are corresponding orbits, identical except for scale, along any line through the intersection of the resonances in Fig. 1, with the coordinates and momenta scaling in proportion to the distance from the intersection and the independent variable (θ) scaling in inverse proportion. Note that this result is rigorous, so long as the motion is adequately described by the Hamiltonian (32), and applies even to features which our analysis is unable to treat. By computing orbits along such a line for various values of α, it is possible to find the distance $(\varepsilon_x^2 + \varepsilon_y^2)^{\frac{1}{2}}$ from the intersection $\nu_x = N/2$, $\nu_y = N/4$ within which $\underline{K}$ represents the motion by comparing the stability limits and other properties of the orbits with the values scaled according to Eq. (30).

IV. COMPUTED ORBIT STUDIES

The motion was studied with the MURA IBM-704 Computer using the ALGYTEE program written by M. Storm [5]. This computer program follows the motion by successively applying the transformation given by Eq. (3).

A series of three points was first examined. The results are given in Table I. The initial conditions were $p_x = 0$, and y, p_y very small. x_t is the value of x at which y growth occurs, and x_s the stability limit above which the motion grows to infinity. For $x_t < x < x_s$, the y amplitude grows to a finite amplitude and declines periodically. The instability for $x > x_s$, is a feature we have not yet treated in our analysis. According to the theorem of corresponding motion, the ratios x_s/x_{sL} and x_t/x_{tL} should be 9, 3, 1. According to the above criteria, point 2 appears to be close enough to $\nu_x = N/2$, $\nu_y = N/4$ so that the other resonance lines were not perturbing the motion appreciably.

TABLE I

	ν_x/N	ν_y/N	$\frac{\nu_x}{N} - \frac{1}{2}$	$\frac{\nu_y}{N} - \frac{1}{4}$	$\frac{\nu_x - \frac{1}{2}N}{(\nu_x - \frac{1}{2}N)_2}$	x_s	$\frac{x_s}{x_{s2}}$	x_t	$\frac{x_t}{x_{t2}}$
L	0.2100	0.1150	− 0.2300	− 0.1350	9	0.496	3.9	0.331	9.5
2	0.4230	0.2048	− 0.0770	− 0.0452	3	0.400	3.2	0.110	2.3
1	0.4744	0.2350	− 0.0256	− 0.0150	1	0.126	1.0	0.0348	1.0

The point L was examined by L. J. Laslett[6]. For this point, x_s is very uncertain since the motion for this point is very erratic. A very small change in the initial conditions leads to very large and very erratic changes in the number of sectors for which the motion is stable. This may be because the point is almost as close to the resonances $\nu_x+2\nu_y=0$ and $\nu_x=0$, as it is to the resonance $\nu_x+2\nu_y=N$. Thus, there are three resonances having nearly equal weight involved in the instability. Point L is almost on the resonance $\nu_x-2\nu_y=0$, which leads to growth, but not in itself to instability. Points 1 and 2 did not have this erratic behavior.

The insert in Fig. 1 shows eight points which were examined with the computer. They are all located on a semicircle at the same distance from $\nu_x=N/2$, $\nu_y=N/4$ as point 2 above. It is clear from the original Hamiltonian (1), and is also a consequence of the theorem of corresponding motions that the equations of motion are invariant under

$$\begin{array}{lll} \nu_x\to-\nu_x & x\to-x & p_x\to p_x \\ \nu_y\to-\nu_y & y\to-y & p_y\to p_y\,. \end{array}$$

Hence there is no additional information to be gained by taking points all the way around $\nu_x=N/2$, $\nu_y=N/4$.

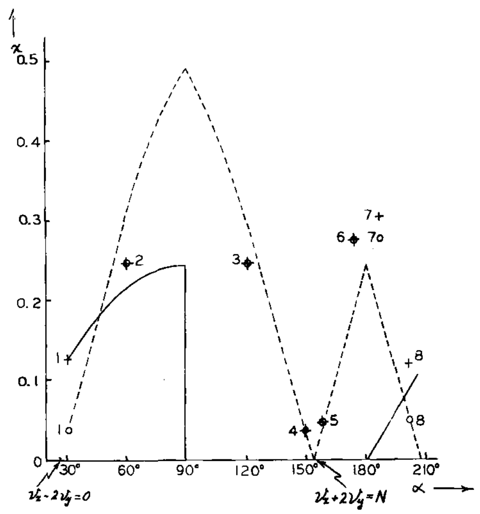

Fig. 3 Stability behavior of computed orbits near the intersection of the resonances $\nu_x-2\nu_y=0$, $\nu_x+2\nu_y=N$. Initial x amplitude is plotted versus angular position α relative to the resonance lines in Fig. 1.
Dashed curves. Predicted threshold x_t for y-growth near difference resonance, and predicted stability limit x_s near sum resonance.
Solid curve. Predicted limiting amplitude x_l below which motion must be stable.
0 Observed threshold for y-growth.
+ Observed stability limit for growth to infinite amplitude.

Table II shows the computed results, and the predicted values for these points. Fig. 3 shows the results in graphic form, plotted as a function of the angle α in Fig. 1.

TABLE II

Point	ν_x/N	ν_y/N	Observed		Theoretical	
			Stability limit	Threshold for y growth	Limit for absolute stability x_l	Threshold of stability limit x_t, x_s
1	0.52502	0.26502	0.126	0.0350	0.124	0.0366
2	0.51493	0.27568	0.249	0.246	0.213	0.303
3	0.48507	0.27568	0.246	—	0.0	0.303
4	0.47439	0.26502	0.0348	—	0.0	0.0366
5	0.47250	0.26101	0.0483	—	0.0	0.0455
6	0.47053	0.25350	0.270	—	0.0	0.186
7	0.47053	0.24650	0.305	0.277	0.0290	0.186
8	0.47250	0.23900	0.112	0.0470	0.0911	0.0455

$$x_t=\frac{4\pi}{\lambda N}|\nu_x-2\nu_y| \qquad \text{for points 1, 2, 7, 8}$$

$$x_s=\frac{4\pi}{\lambda N}|\nu_x+2\nu_y-N| \qquad \text{for points 3, 4, 5, 6}$$

$$x_l=\frac{4\pi}{\lambda N}\left|\nu_y-\frac{N}{4}\right| \qquad \text{for points 1, 2, 7, 8}$$

$$x_l=0 \qquad \text{for points 3, 4, 5, 6}$$

Near the resonances, the analytic (single resonance) formulas for thresholds and stability limits agree well with computed values. Further from the resonances, the agreement is only in order of magnitude, as might be expected. However, the general pattern is clear :

1. In the first and third quadrants (near the difference resonance), the effective stability limit is the greater of x_l or x_t. For point 1, $x_l > x_t$ and x_l is the effective stability limit. For point 2, $x_t > x_l$ and x_t is the effective stability limit. There is reason to believe that if the computer runs could be made long enough, points 7 and 8 would be found to have lower stability limits so that they too may fit into this picture. More will be said about 7 and 8 below.

2. If $x_t < x_l$, the y-amplitude grows to a finite amplitude and oscillates when $x_t < x < x_l$, while for $x_t > x_l$ y-growth leads to instability.

3. In the second and fourth quadrants (near the sum resonance) the theoretical stability limit x_s is the effective stability limit.

These results are consistent with the analytic theory. Near the sum resonance the analytic theory considering the sum resonance alone seems to give an adequate and complete treatment of the motion. Although it is " energetically " possible for the particle to escape, it does not in fact do so because there is another approximate constant of the motion (ρ_2) which prevents the particle from following the energy surface to infinity except when the stability limit is exceeded. Presumably the stability for $x < x_s$, at least well inside the second and fourth quadrants, should be as good as stability of non-linear motions in general as predicted by the Moser-Birkhoff methods. Experimentally, we find that for one-dimensional motion, orbits within predicted stability limits are so stable, at least for the numbers of sectors we can now compute in a reasonable time ($\sim 10^6$), that they do not deviate perceptibly (i.e. within as much one part in 10^5) from closed phase curves. For two-dimensional motion the orbits also appear stable for many sectors, but it is impossible to obtain as precise a measure of the stability because the phase motion is in four dimensions.

Near the difference resonance, our computed results are consistent with, but go beyond the analytic theory, and seem to suggest the following picture. Below the theoretical limit of stability x_l, the motion is certainly stable, at least for very long times, and can be adequately accounted for by the analytic theory of the difference resonance alone, which gives a complete description of the motion. Above the limit x_l, it is energetically possible for the particle to escape to infinity, but it will not in fact do so if we are below the threshold for coupling because the analytic theory, which should give a correct description at least for very long times, predicts that the particle remains near the x-axis and hence never arrives in the vicinity of the pass. However, above the coupling threshold, the particle wanders all over the energy surface, and hence finds its way out of the pass and escapes. One consequence of this picture is that when $x_t > x_l$, a particle with x slightly greater than x_t has an energy well above the minimum ($-\frac{1}{2} K_l$) to cross the pass, and hence should quickly find its way out since the opening available is large. However, if $x_t < x_l$, a particle with x slightly greater than x_l has only barely enough energy to escape and must therefore strike the pass very accurately to escape. This is confirmed in part by the results which show that when $x_t > x_l$, the particle usually escapes quickly if $x > x_t$, whereas if $x_t < x_l$ and x is slightly above x_l, the y-amplitude may grow and oscillate regularly a few times and even many times before suddenly going off to infinity. (By " infinity " we mean an amplitude large in comparison with the stable motion; the distinction is always very clear in that the particle coordinates all increase very rapidly when the motion becomes unstable). This phenomenon is illustrated by the behavior at point 8 discussed below.

Results of computed orbits for point 2 with initial conditions $p_x = p_y = 0$, $y = 10^{-8}$, $x = 0.248$ and 0.250, and for point 8 with initial x of 0.108, 0.116, 0.125, 0.133 are given in Table III.

TABLE III

Point	x Initial	Number of sectors before going unstable
2	0.250	1,745
	0.248	still stable at 10^6 sectors
8	0.166	1,066
	0.133	6,671
	0.125	36,049
	0.116	346,620
	0.108	still stable at 10^6 sectors

The stability limit for point 8 is not as sharply defined as that of point 2. If a series of computer runs of 25,000 sectors were made for various values of initial x, and a second series of 10^6 sector runs were made, for point 2 one would find $0.248 < x_s < 0.250$ for both runs while for point 8 very different values would be found. If one could make runs of 10^9 sectors at point 8, x_s might be found to be much lower than the value given here. Points 1 through 6 behaved as point 2 above, and 7 and 8 like point 8. The behavior of point 7 is anomalous in view of the discussion above.

Point 8 shows the inadequacy of trying to study coupling resonances with runs of only a few hundred sectors.

In addition to the phenomena discovered here, which depend only on the two resonances, we may expect that if we move farther from the resonance, additional effects due to other resonances will arise. The neglected terms can be shown to cause rapid oscillations in the " constants " $\underline{K}$, ρ_2, etc., and when there are many of these, one might expect random fluctuations in their values. This would make predicted stability limits fuzzy and give rise to erratic behavior such as that observed by Laslett for point L (Table I). Note that this behavior is not what we have observed for point 8, although it resembles it, because point L is on the same ray, very nearly, as our point 1 which showed no such behavior; so that the erratic behavior at point L is a violation of the theorem of corresponding motions and must be due to neglected resonance terms.

LIST OF REFERENCES

1. See for example: Hagedorn, R. Stability of two-dimensional non-linear oscillations with periodical Hamiltonian applied to betatron oscillations in circular particle accelerators. Part I and II. CERN (*) 57-1. 7th March, 1957.
2. Hagedorn, R. Note on an instability on a difference resonance line. CERN Symp. 1956. *1*, p. 293-4.
3. Laslett, L. J. and Symon, K. R. Particle orbits in fixed field alternating gradient accelerators. CERN Symp. 1956. *1*, p. 279-89.
4. Moser, J. Stabilitätsverhalten kanonischer Differentialgleichungssystems. Nachr. Akad. Wiss. Göttingen. Math. Phys. Kl. 1955. p. 87-120.
5. Storm, M. R. ALGYTEE (Program 58) MURA (*) 233. March, 1957.
6. Laslett, L. J. Computational examples of solutions to differential equations which simulate growth of axial oscillations in an FFAG accelerator operated near the $\sigma_x = 2\sigma_y$ resonance. MURA (*) 295, June 7, 1957.

DISCUSSION

WALKINSHAW: If $\nu_x = \frac{1}{2}N$ at the junction, then the mode number would be equal to π and you would not get stable operation.

SYMON: That is correct. In an actual accelerator one would not be operating in this region and one would want to consider other resonance crossings. However, it happened to be convenient to pick this particular resonance intersection for this study because it was easy to treat analytically. In our study the linear resonance $\nu_x = \frac{1}{2}N$ does not occur because we put constant coefficients in the linear terms.

PENTZ: I would like to ask in relation to the longitudinal instabilities that you discussed in the latter part of your talk, what you consider happens next in the situation where the energy spread, for instance in your 2 MeV beam (we would have the same situation in our 2 MeV beam) is less than the amount required for stability. The theory suggests that longitudinal instabilities will begin to build up. Does the situation then become non-linear and does the theory cover what happens next?

SYMON: I should say the simplest answer to this question is that we do not know. We have looked at this in two ways. We have attempted to solve the Boltzmann equation by digital computation, but the results are not yet satisfactory. We also have a hand-waving argument about what happens in the non-linear region, which is sufficiently good that we can predict the critical energy spread correctly. If this argument is correct, it would lead one to the conclusion that if the actual energy spread is not too far below this limit, the amplitude should grow to some predictable value and then not grow any further. However, as I say, we have no computations which suggest that this is the case. The few computations we do have suggest the reverse; that is, we have never seen the motion stop growing.

KOLOMENSKIJ: In relation with the upper limit for instability mentioned at the end of Symon's report I should like to ask whether it is of practical importance or not. I have also a question about the non-linear effects. In your work and in the work Lebedev and I have carried out we have considered only linear effects; does this seem justified to you?

SYMON: I think I can answer the second question first by saying that we really do not yet know anything about non-linear effects. The first question, I believe, referred to the instabilities of the cavity modes that I spoke about at the end. At first we tried to prove that the electromagnetic modes were always stable and we found we could prove this if we assumed that the angular velocity of the electromagnetic mode in the empty cavity is greater than c/R where R is the radius of the particle. However, it now turned out just recently that this condition is not satisfied in a circular cavity; for any R which lies inside the cavity, there is always some electromagnetic mode which propagates with the velocity slower than c/R and the only thing I can say is that the proof that the electromagnetic modes are stable then breaks down. We have no definite results, but if you look at the formulae you see that one could then have instabilities of the electromagnetic modes under certain conditions, but we do not know precisely what those conditions are.

(*) See note on reports, p. 696.

KITAGAKI: My question does not pertain directly to this report. In the table of Jones' report in Session I, a stored current of for instance 800 A - 100 A was mentioned; if we consider the space-charge effects in cross-over points, I cannot think of such a big storage current.

SYMON: If you refer to the instability above the transition energy, then the limiting energy spread depends on the square root of the number of particles, whereas the actual energy spread of the beam as a consequence of Liouville's therorem is proportional to the number of particles. Consequently, the conditions for stability improve if you stack a larger beam because the energy spread of the beam increases faster than the critical energy spread. So, curiously enough, it turns out that the most critical case is the case of the single beams that are being accelerated and not the stacked beam. The more beam you stack, the more stable it becomes.

LAWSON: I wonder if you could tell me how these considerations apply to the operation of proton colliding beam systems. Have you put the numbers in for these?

SYMON: I do not recall any precise numbers. I do know that in almost every other case that we looked at, except the model which we have under construction, the condition for stability seems to be satisfied.

NON-LINEAR THEORY OF BETATRON OSCILLATIONS (*)

Yu. F. Orlov and E. K. Tarasov

Physical Institute of the Armenian Academy of Sciences, USSR

(presented by D. G. Koshkarev)

We consider parametric resonances (that is resonances caused by a variation of the parameters of the machine) resulting from the coupling of synchrotron and betatron oscillations and also so-called cylindrical resonances, that is resonances on a difference line, when there is an exchange of energy between the r- and the z-directions.

I. APERTURE NARROWING NEAR RESONANCES

As has already been shown [1-3], the motion of particles near the resonances can be described in a Hamiltonian form with canonical variables A^2 (generalized momentum) and χ (**) (generalized coordinate) where A is a particle oscillation amplitude (see Eq. 1.16) (***) and χ is a beating phase Eq. (1.9) (1.10).

For the analysis of motion it is sufficient to know the first integral $H(A^2, \chi)$ by means of which the adiabatic invariant J can be found:

$$J = \oint p dq = \oint A^2 d\chi \qquad (2.1)$$

Near the resonances the oscillation amplitude depends on time. Beatings which are characteristic for resonances are depicted on (A^2, χ) plane as phase diagrams (Figs. 3, 4, 5, 6, 7, 13, 14, 15). The adiabatic integral is equal either to the phase diagram area within the limits of 0 to 2π provided the diagram is not closed, or to the area encircled by a closed phase diagram. Far from resonances the amplitude is constant and the adiabatic invariant is

$$J_\infty = 2\pi A^2 \qquad (2.2)$$

If A is the maximum amplitude possible in the accelerator chamber and J is a near-resonance

(*) This paper represents the second part of a communication of which the first appeared in Nuovo Cimento [1].

(**) In a previous paper [1] the same letter φ was used to denote both phase variable and Floquet's function as a results of the authors' carelessness. (Yu. F. O. and E. K. T,)

(***) Binary numeration of formulae is used the first figure is a part number and the second figure is a formula number.